

Cranial shape transformation in the evolution of the giant panda (*Ailuropoda melanoleuca*)

Borja Figueirido · Paul Palmqvist ·
Juan A. Pérez-Claros · Wei Dong

Received: 17 August 2010 / Revised: 16 November 2010 / Accepted: 17 November 2010 / Published online: 4 December 2010
© Springer-Verlag 2010

Abstract In this study, landmark-based methods of geometric morphometrics are used for investigating the main aspects of cranial shape transformation in the evolution of the giant panda, *Ailuropoda melanoleuca*. Specifically, we explore if the highly derived cranial adaptations for bamboo feeding of the living panda were developed early in the panda's lineage. Results obtained show that the overall cranial morphologies of the oldest known panda, the “pygmy” *Ailuropoda microta*, and the late Pleistocene *Ailuropoda baconi* are both very similar to that of their closest living relative, *A. melanoleuca*, which agrees with a previous proposal based on qualitative criteria. However, we also describe several differences between the crania of *A. microta*, *A. baconi*, and *A. melanoleuca*, including the development of the postorbital process, the orientation of the occipital region, and the expansion of the braincase. As a result, the cranial morphology of *A. microta* shows a less specialized morphology toward a fibrous and durophagous diet compared to the giant panda. These results are confirmed by a comparative analysis of the dimensions of the upper teeth in bears, which has revealed differences in relative tooth size between *A. microta* and *A. melanoleuca*, most probably as a result of mosaic evolution. Therefore, we conclude that cranial shape did not remain essentially uniform in the

Ailuropoda lineage, as previously thought, but underwent a number of changes during more than 2 Myr.

Keywords *Ailuropoda* · Cranial morphology · Evolution · Geometric morphometrics

Introduction

The evolutionary history of the giant panda, *Ailuropoda melanoleuca*, has been debated for decades and is still a matter of controversy today. The central core of the debate lies in the phylogenetic relationships of *Ailuropoda*, an issue that is not clarified by the scarce fossil record available for the panda lineage (Bininda-Emonds 2004; Hunt 2004; Jin et al. 2007). Recent phylogenetic studies based on both molecular and morphological data indicate that *Ailuropoda* represents a sister lineage to all living ursids, with the highly specialized morphology of this genus resulting from its peculiar diet based on bamboo (Flynn and Nedbal 1998; Wyss and Flynn 1993; Gittleman 1994; Bininda-Emonds et al. 1999; Krause et al. 2008). The poor evidence from the fossil record supports the ursid affinities of *Ailuropoda*: dental remains of the late Miocene *Ailurarctos yuanmouensis* and *Ailurarctos lufengensis* (Yunnan province, China; Qiu and Qi 1989; Hunt 2004; Qi et al. 2006) show that the giant panda lineage most probably originated from the Holarctic genus *Ursavus* at some time during the Miocene (Hunt 2004). A number of dental traits shared with the Miocene *Ursavus* evidence the ursid affinities of *Ailurarctos*, including (1) the retracted internal cusp (protocone) of the upper carnassial (P4); (2) the migration of the metaconule to the posterointernal corner of the upper first molar (M1), which gives this tooth a square shape; (3) the addition of the talon of the second

B. Figueirido (✉) · P. Palmqvist · J. A. Pérez-Claros
Área de Paleontología, Departamento de Ecología y Geología,
Facultad de Ciencias, Universidad de Málaga, Campus
Universitario de Teatinos,
29071 Málaga, Spain
e-mail: Francisco.figueirido@uv.es

W. Dong
Institute of Vertebrate Paleontology and Paleoanthropology,
Chinese Academy of Sciences,
100044, Beijing, China

molar (M2) to its posterior border; and (4) the broad, expanded enamel crowns of the second and third lower molars (m2 and m3, respectively), typical of ursine bears (Hunt 2004). In addition, *Ailurarctos* shares also some morphological specializations with the living panda, for example, (1) the expanded upper and lower molars (M1-2 and m2-3, respectively), (2) the wrinkled crowns of the molars, and (3) an incipient addition of accessory cusps to the premolars (Hunt 2004). Therefore, *Ailurarctos* represents the first and most feasible member of the *Ailuropoda* lineage and, strikingly, its dental morphology suggests an incipient crushing dentition toward a durophagous diet (Hunt 2004; Jin et al. 2007).

The late Pliocene species *Ailuropoda microta* and *Ailuropoda wulingshanensis* have intermediate dental morphologies between those of the Miocene *Ailurarctos* and the living *A. melanoleuca* (Jin et al. 2007). Therefore, dental traits apparently reveal that the giant panda lineage evolved from a stem precursor stage during the Miocene toward the more complex cusped teeth and grinding occlusal pattern of the living giant panda (Jin et al. 2007). However, the specialized diet of *Ailuropoda* entails extensive morphological specializations in both the cranium and mandible other than the presence of complex, cusped teeth (Sacco and Van Valkenburgh 2004; Christiansen 2007; Figueirido et al. 2009; Meloro et al. 2008; Figueirido and Soiblezon 2010).

In this paper, we explore cranial shape transformation in the evolution of the ailuropodine lineage using landmark-based geometric morphometrics. Specifically, we investigate (1) if skull shape transformation in the evolution of *Ailuropoda*, and its concomitant specialized diet, was attained at an early stage in the evolutionary history of ailuropodines and remained uniform for more than 2 Myr, as proposed by Jin et al. (2007); or (2) if the complex skull morphology of *Ailuropoda* is a more recent phenomenon, as indicated by dental morphology.

Materials and methods

Data

Shape data were collected for 171 crania belonging to all living bear species (Table 1). Only adult specimens were used for the analyses to avoid the effects of ontogenetic variation. Similar numbers of males and females of each living species and similar proportions of individuals from different populations were sampled whenever possible. Specimens were photographed and measured at the American Museum of Natural History (New York, NY, USA), the Natural History Museum (London, UK), and the Museum für Naturkunde (Berlin, Germany).

Table 1 Sample sizes (*N*, lateral/dorsal/ventral) for the crania of living bear species used in the morphometric analyses

Species	Common name	<i>N</i>
<i>Ailuropoda melanoleuca</i>	Giant panda	14/17/18
<i>Tremarctos ornatus</i>	Andean spectacled bear	9/8/12
<i>Ursus ursinus</i>	Sloth bear	24/27/27
<i>Ursus arctos</i>	Brown bear	28/23/37
<i>Ursus americanus</i>	North American black bear	10/7/7
<i>Ursus maritimus</i>	Polar bear	21/21/28
<i>Ursus malayanus</i>	Malayan sun bear	16/18/17
<i>Ursus thibetanus</i>	Asian black bear	17/20/25

In order to describe cranial shape transformation in the giant panda lineage, two specimens of two extinct species of *Ailuropoda* were included in the analysis: *A. microta* (IVPP V14564) and *Ailuropoda baconi* (IVPP V5038) from the late Pliocene and the late Pleistocene of China (Dong 2008), respectively. Fossil skulls of Miocene *Ailurarctos* and of Plio-Pleistocene *A. wulingshanensis* are either incomplete or badly preserved. As a result, these species were not considered in the analyses.

Landmark digitalization

A total of 38 landmarks (16, 10, and 12 taken in the lateral, dorsal, and ventral views, respectively) were digitized with program TPSdig v. 2.05 (Rohlf 2006) from high-resolution digital photographs of the bear crania (Fig. 1 and Table 2). All the photographs were collected with a tripod and following a standardized protocol for avoiding lens distortion and parallax (Meloro et al. 2008).

A major limitation of using landmark-based methods with fossils is that well-preserved, undeformed, and complete specimens are required (Slater and Van Valkenburgh 2008). This precluded collecting morphological information from the zygomatic arches of ailuropodines because some fossils do not preserve these bones. However, special attention was paid to digitizing landmarks (LMs) that accurately describe key functional features of the bear skull, including snout length (LMs 1–9 in lateral view, LMs 1 and 2–3 in dorsal view; Fig. 1a, b), the position and size of the glenoid fossa (LMs 6–7 in lateral view; Fig. 1a), the position of orbits (LMs 8–9 in lateral view; Fig. 1a), the mesiodistal length of the upper molar tooth row (LMs 14 and 16 in lateral view; Fig. 1a), the area of the temporal fossa (LMs 2–3, 4, and 8 in lateral view; Fig. 1a), the angle between the occiput and the upper tooth row (LMs 3–4 and 16–11 in lateral view; Fig. 1a), the maximum width of the braincase (LMs 8–9 in dorsal view; Fig. 1b), cranium width measured over the zygomatic arches (LMs 6–7 in dorsal view; Fig. 1b) and over the postorbital process (LMs 4–5 in dorsal view;

Fig. 1 Landmarks used in the morphometric analysis of bear crania in lateral (a), dorsal (b), and ventral (c) views. For the anatomical criteria used in the selection of landmarks, see also Table 2. The cranium illustrated is a specimen of *A. melanoleuca* (AMNH-89028)

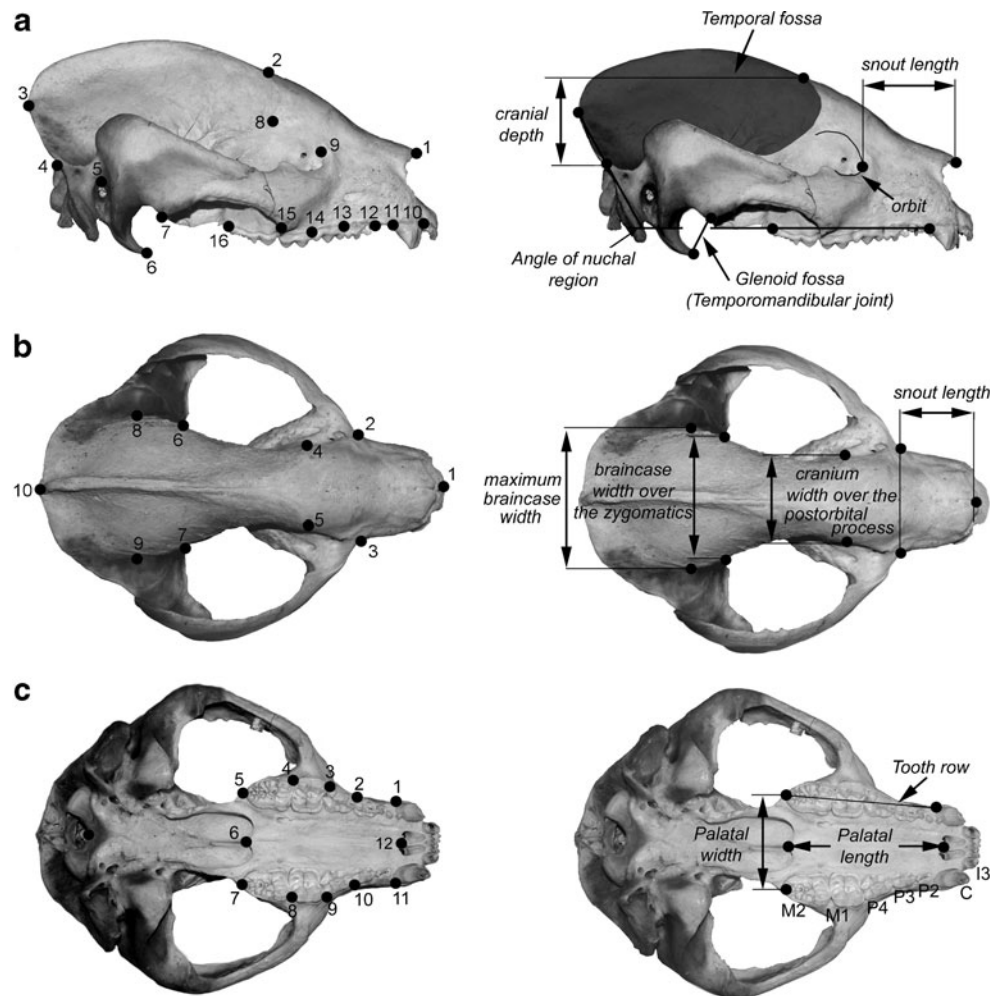


Fig. 1b), palatal length (LMs 6–12 in ventral view; Fig. 1c), and palatal width over the posterior end of the tooth row (LMs 5–7 in ventral view; Fig. 1c).

Multivariate analyses

The specimens were aligned using the Procrustes method (Dryden and Mardia 1998) for the three views separately. A multivariate regression analysis (Monteiro 1999) of shape (i.e., Procrustes coordinates) on size (i.e., log-transformed centroid size) was computed for exploring the effects of size on shape variation. The statistical significance of the regressions was checked with a permutation test against the null hypothesis of independence (Drake and Klingenberg 2008). Principal components analyses were performed on the covariance matrix of the aligned coordinates for both samples separately. Given that this study does not focus on the degree of cranial bilateral asymmetry, the covariance matrices for the analyses in dorsal and ventral views were computed using only the symmetric component of shape variation (Klingenberg et al. 2002). All morphometric

procedures and statistical analysis were performed with MORPHOJ software package (Klingenberg 2011).

Analysis of tooth dimensions

In order to test the degree of dental specialization in the pygmy *A. microta*, tooth dimensions were calculated in both extant bears and extinct ailuopodines. Specifically, the maximal anteroposterior and lateromedial tooth diameters of all specimens sampled per species were averaged. As a result, the square root of the anteroposterior length multiplied by the lateromedial width of each tooth was computed. These values were divided by skull length and used as proxies for relative tooth size in each bear species.

Results

The multivariate regressions of the symmetric component of shape on the log-transformed values of centroid size were significant ($p < 0.0001$) for the three views of the

Table 2 Landmarks used in the morphometric analyses of the bear crania

Lateral view	
1	Most anterior edge of the nasal bones
2	Dorsal outline directly superior to the post-orbital process
3	Most postero-ventral point of the occipital crest
4	Intersection between the occipital condyle and the occiput
5	Most dorsal point of external acoustic meatus (i.e., ear canal)
6	Ventral tip of postglenoid process
7	Ventral tip of preglenoid process
8	Tip of postorbital process
9	Position of the orbit at half height
10	Most antero-dorsal border of the canine alveolus
11	Most postero-dorsal border of the canine alveolus
12	Anterior edge of the upper tooth row
13	Interdental gap between the upper carnassial and the third premolar
14	Interdental gap between the first upper molar and the upper carnassial
15	Ventral intersection between the zygomatic arch and the maxilla
16	Posterior edge of the upper tooth row
Dorsal view	
1	Prosthion
2	Intersection between the left zygomatic arch and the maxilla
3	Intersection between the right zygomatic arch and the maxilla
4	Tip of the left postorbital process
5	Tip of the right postorbital process
6	Intersection between the left zygomatic arch and the braincase
7	Intersection between the right zygomatic arch and the braincase
8	Point of maximum curvature on the left side of the braincase
9	Point of maximum curvature on the right side of the braincase
10	Tip of the occipital crest
Ventral view	
1	Most posterior point of the left canine alveolus
2	Interdental gap between the left third and fourth premolars
3	Interdental gap between the left fourth premolar and first molar
4	Interdental gap between the left first and second molars
5	End of the left third molar
6	Most posterior point between the two palatine bones
7	Posterior end of the right third molar
8	Interdental gap between the right first and second molars
9	Interdental gap between the right fourth premolar and first molar
10	Interdental gap between the right third and fourth premolars
11	Most posterior point of the right canine alveolus
12	Point between the two incisive foramina

cranium (i.e., lateral, dorsal, and ventral). The total amount of shape variation that accounted for size differences was 17.8% in the ventral view, 21.8% in the dorsal view, and 8.3% in the lateral view.

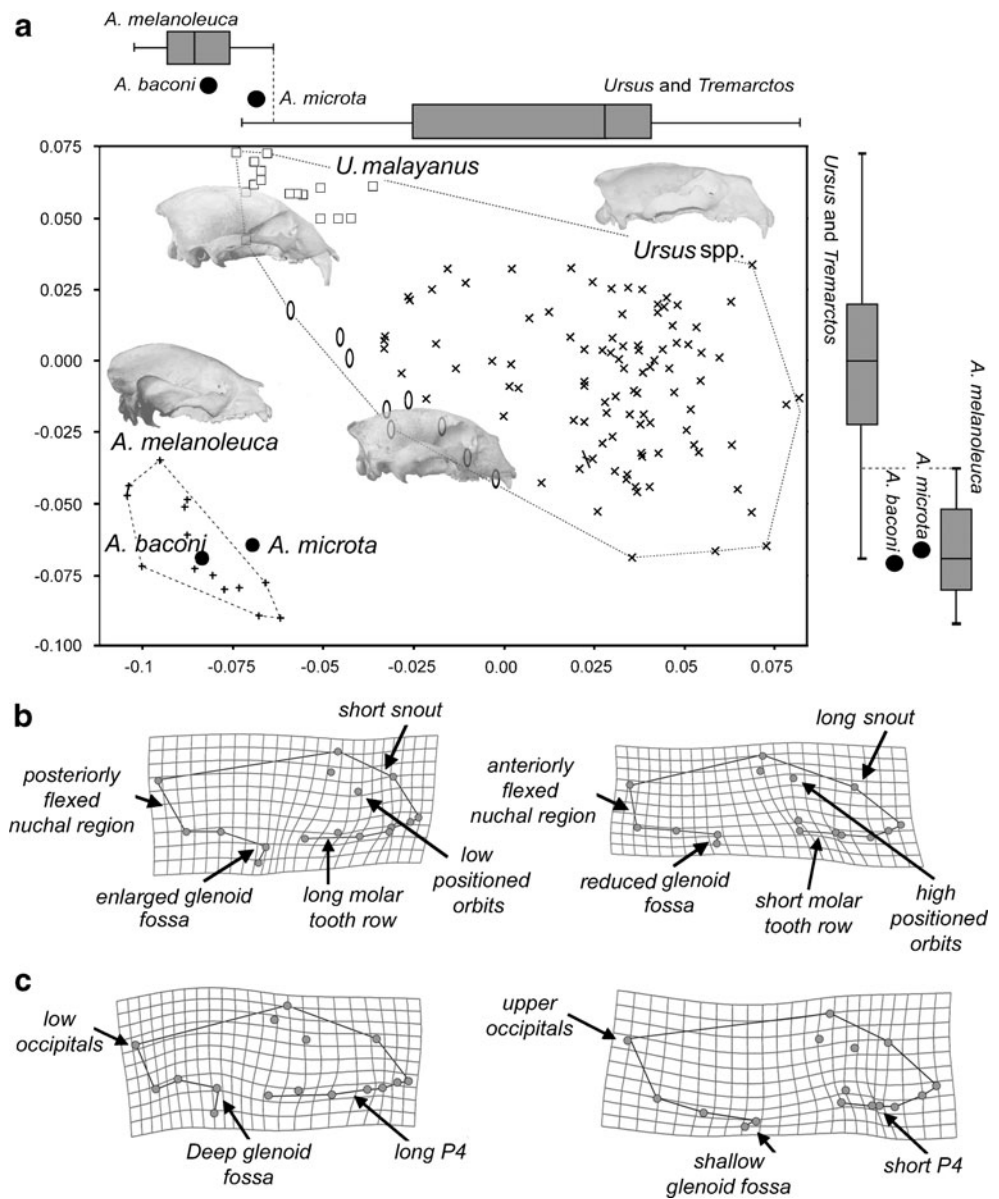
Analysis of bear crania in lateral view

Figure 2a shows the morphospace defined by the first two principal components (PCs) derived from the analysis of

bear crania in lateral view. The first PC (36.7% of the original variance in landmark positions explained) mainly separates ailuropodines (*A. melanoleuca*, *A. baconii*, and *A. microta*) and, to a lesser extent, the sun bear (*Ursus malayanus*) from the other ursids included in the analysis (Fig. 2a, *x*-axis). The second PC (23.0% of the variance accounted) basically reflects the morphological differences between the crania of sun bears, which score with extreme positive values, and those of giant pandas, which take the

Fig. 2 Multivariate analyses of cranial shape in lateral view for extant and extinct bears.

a Morphospace defined by the first two PCs. *Boxplots* of the species scores on each PC are also shown for clarity. The vertical line inside each box is the median. Box length is the interquartile range (IQR) and shows the difference between the 75th and 25th percentiles. Horizontal bars enclose values of 5–95%. **b** Shape changes accounted for by the first PC. **c** Shape changes accounted for by the second PC. Symbols: *x*, *Ursus* spp. (except *U. malayanus*); ovals, *Tremarctos*; crosses, *Ailuropoda*; squares, *U. malayanus*. Units in the *x*- and *y*-axes are factor scores



lowest negative scores (Fig. 2a, *y*-axis). Therefore, it is the combination of both PCs which allows defining the range of shape variation in both the extant and extinct ailuropodines.

Figure 2b and c include thin plate spline (TPS) diagrams that describe the shape changes accounted for by the first and second PCs, respectively. These diagrams show that the panda's cranium has a snout that is short and deep (i.e., high across the dorso-ventral axis), a large and deep glenoid fossa, a low positioned occipital and orbits, a posteriorly flexed nuchal region, a long molar tooth row, and an enlarged fourth premolar (Fig. 3b, c).

Strikingly, the cranium of the earliest panda, the pygmy *A. microta* from the Late Pliocene of China, plots in the morphospace within the range of shape variation of *A. melanoleuca* (Fig. 2a). This shows that the overall

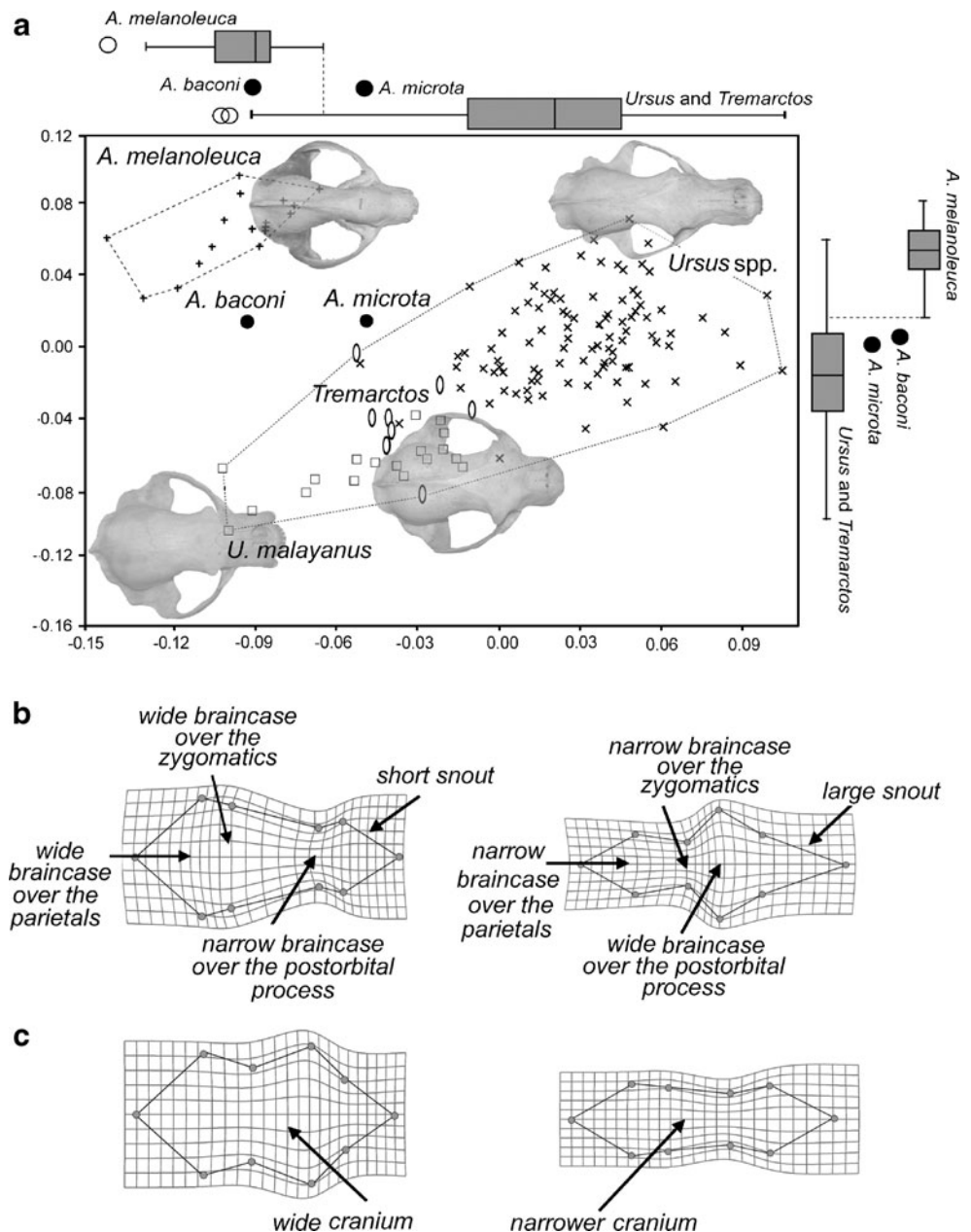
cranial morphology in lateral view of this primitive panda is very close to that of the living giant panda. In fact, the TPS diagrams show a set of ailuropodine traits in the cranium of *A. microta*, including a long temporal fossa, an enlarged and deep glenoid fossa, and a brachycephalic (i.e., short-snouted) condition. However, the fact that *A. microta* plots outside the interquartile range of shape variation for *A. melanoleuca* (Fig. 2a) in the first PC indicates the less marked ailuropodine morphology of the cranium of the pygmy panda, which is reflected in a comparatively shorter molar tooth row and, specially, a shorter fourth premolar. In addition, *A. microta* shows a less anteriorly flexed nuchal region and a shorter snout than the giant panda. In contrast, the cranium of *A. baconii* is, in general terms, indistinguishable from the one of *A. melanoleuca*.

Analysis of bear crania in dorsal view

Figure 3a shows the morphospace defined by the first two PCs derived from the analysis of bear crania in dorsal view. The first PC (42.3% of variance explained) mainly separates the two giant pandas, *A. melanoleuca* and *A. baconi*, plus *U. malayanus* from *A. microta* and the other living bears (Fig. 3a, x-axis). The second PC (26.1% of the variance accounted for) basically separates the specimens of *U. malayanus*, which take extreme negative values, from the living giant pandas, which score with the highest positive values (Fig. 3a, y-axis). Figure 3b and c show TPS diagrams that describe the shape changes accounted for by the first and second PCs.

As in the case of the analysis of cranial shape in lateral view, it is the combination of the specimens' scores on both PCs which defines the range of shape variation in both the extant and extinct ailuropodines (Fig. 3a). TPS diagrams show that compared to other bears, the cranium of the giant panda has a short snout and a wide braincase, and is comparatively narrower over the postorbital process but wider over the zygomatic arches (Fig. 3b). Strikingly, *A. microta* shows an intermediate cranial morphology in dorsal view between *A. melanoleuca* and the other living bears (Fig. 3a, boxplots). As a result, the cranium of the pygmy panda is wider over the postorbital process and the zygomatic arches than in the

Fig. 3 Multivariate analyses of cranial shape in dorsal view for extant and extinct bears. **a** Morphospace defined by the first two PCs. Boxplots of the species scores on each PC are also shown for clarity. **b** Shape changes accounted for by the first PC. **c** Shape changes accounted for by the second PC. For symbols, see Fig. 2. Units in the x- and y-axes are factor scores

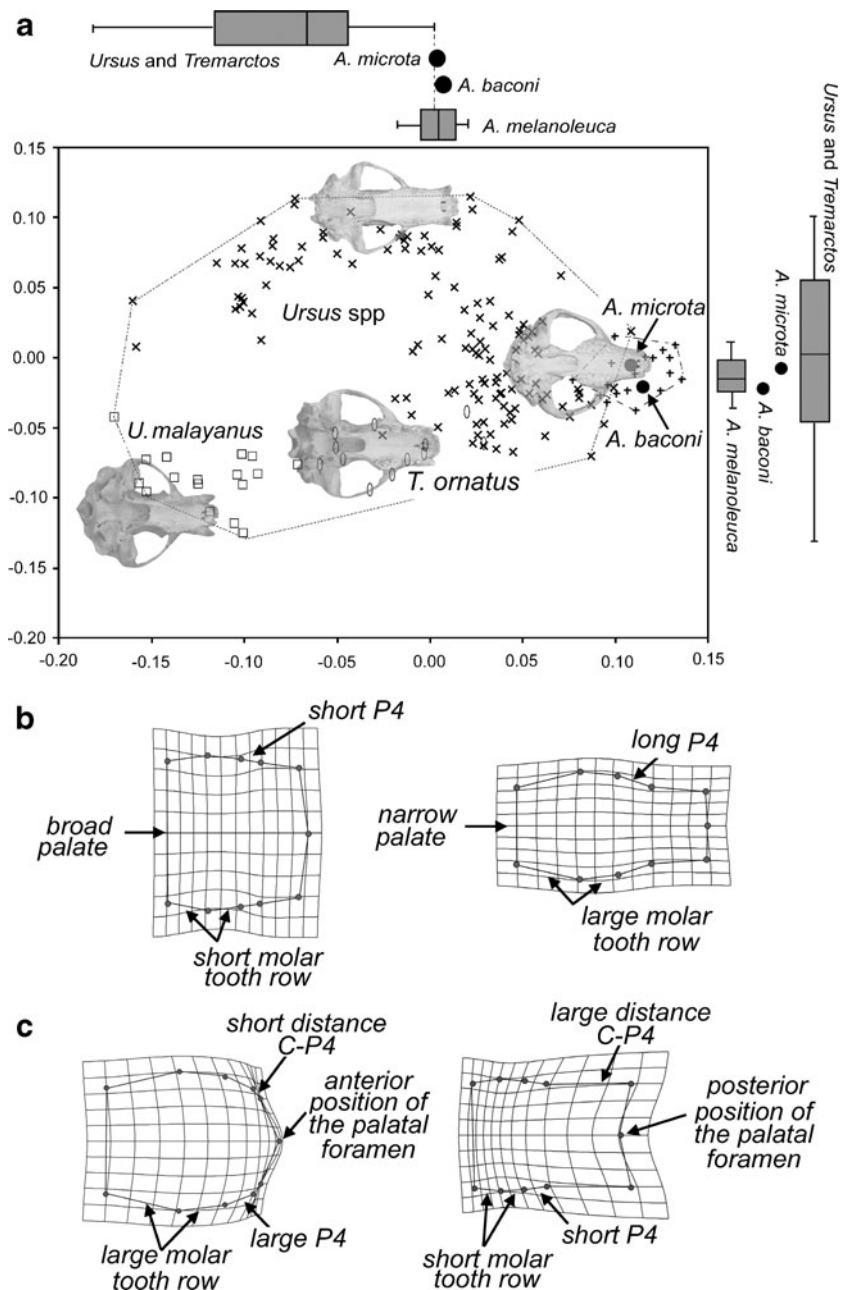


case of the giant panda, and also has a narrower braincase. In contrast, the cranium of *A. baconi* lies within the range of shape variation in PCI scores for the specimens of *A. melanoleuca* (Fig. 3a, PCI-boxplot), although it overlaps also with the lower range of shape variation in PCII scores for *Ursus* and *Tremarctos* (Fig. 3a, PCII-boxplot). Therefore, these results show that *A. baconi* has a braincase that is wider than in *Ursus* spp. and *Tremarctos*, and a cranium that is broader over the postorbital process and the zygomatic arches than in half of the specimens of *A. melanoleuca*.

Analysis of bear crania in ventral view

Figure 4a shows the morphospace defined by the first two PCs derived from the analysis of bear crania in ventral view. The first PC (51.4% of variance explained) mainly separates both extant and extinct ailuropodines from other living bear species (Fig. 4a, x-axis). The second PC (21.2% of the variance explained) tends to separate the specimens of *U. malayanus*, which take extreme negative values, from other living bear species, which score with highest positive values (Fig. 4a, y-axis). Figure 4c and d show TPS

Fig. 4 Multivariate analyses of cranial shape in ventral view for extant and extinct bears. **a** Morphospace defined by the first two PCs. *Boxplots* of the species scores on each PC are also shown for clarity. **b** Shape changes accounted for by the first PC. **c** Shape changes accounted for by the second PC. For symbols, see Fig. 2. Units in the x- and y-axes are factor scores



diagrams that describe the shape changes accounted for by the first and second PCs, respectively.

In contrast to previous analyses, in this case, it is only the specimens' scores on the first PC which defines the range of shape variation in both the extant and extinct ailuropodines (Fig. 4a, boxplots). TPS diagrams show that compared to other bears, the palate of ailuropodines is narrow and large, has long molar tooth rows, and enlarged fourth premolars (Fig. 3b). Strikingly, the palatal morphology of both extinct ailuropodines, *A. microta* and *A. melanoleuca*, is indistinguishable from the one of *A. melanoleuca* (Fig. 4a, boxplots).

The second PC does not distinguish the palatal morphology of ailuropodines from those of other bears (Fig. 4a, PCII-boxplots). In contrast, this PC mainly separates the palatal shape of *U. malayanus* from other bear species, showing that the sun bear has an extremely wide and short palate, a short distance between the canine and the fourth premolar, a longer molar tooth row, and a more enlarged fourth premolar.

Discussion

Contrary to Jin et al. (2007), this study shows that cranial shape did not remain essentially uniform in the giant panda lineage for more than 2 Myr. In fact, the cranial morphology of the late Pliocene *A. microta* is intermediate between other ailuropodines and the rest of the living bear species. In addition, a shape gradient can be traced from the primitive *A. microta* to the extinct *A. baconi* and the living *A. melanoleuca*. Thus, our results indicate that the cranial morphology of the living giant panda evolved at an early stage in the Miocene, most probably from *Ailurarctos*, following a trend through the late Pliocene *A. microta*

toward the more derived shape of *A. melanoleuca*. Therefore, *A. microta* and, to a lesser degree, *A. baconi* represent intermediate stages for cranial shape transformation in *Ailuropoda*. In fact, the cranium of *A. microta* has an incipient development of some characters that were well established in the extinct *A. baconi* and show an extreme condition in the living *A. melanoleuca*. This is evidenced by the wider cranium over the postorbital process and zygomatic arches of the pygmy panda, as well as by the presence of a narrower braincase, a relatively longer snout, and an anteriorly less flexed nuchal crest than in *A. melanoleuca*. It is worth noting that this result is confirmed by a comparative analysis of the dimensions of the upper teeth in bears (Fig. 5). In fact, the dimensions of the canine of *A. microta* and the other ailuropodines are identical to those of *Ursus* and *Tremarctos*, while the relative size of the first molar of the pygmy panda is intermediate between *A. melanoleuca* and *A. baconi*, on the one hand, and *Ursus/Tremarctos*, on the other. In contrast, the dimensions of the fourth premolar of *A. microta* are closer to the other ailuropodines. Such differences in tooth size suggest a pattern of mosaic evolution. Therefore, the upper second molar of the pygmy panda did not attain the extreme degree of development present today in *A. melanoleuca* or in the late Pleistocene *A. baconi*.

There is a close association between cranial morphology and feeding behavior in bears (Sacco and Van Valkenburgh 2004; Figueirido et al. 2009, 2010; Figueirido and Soiblezon 2010). For this reason, it is reasonable to infer that the morphological resemblance between *A. microta* and the living *A. melanoleuca* reflects a similar feeding behavior. In fact, a brachycephalic skull with a large temporal fossa, long molar teeth, and an enlarged post-glenoid process is well adapted towards a durophagous diet

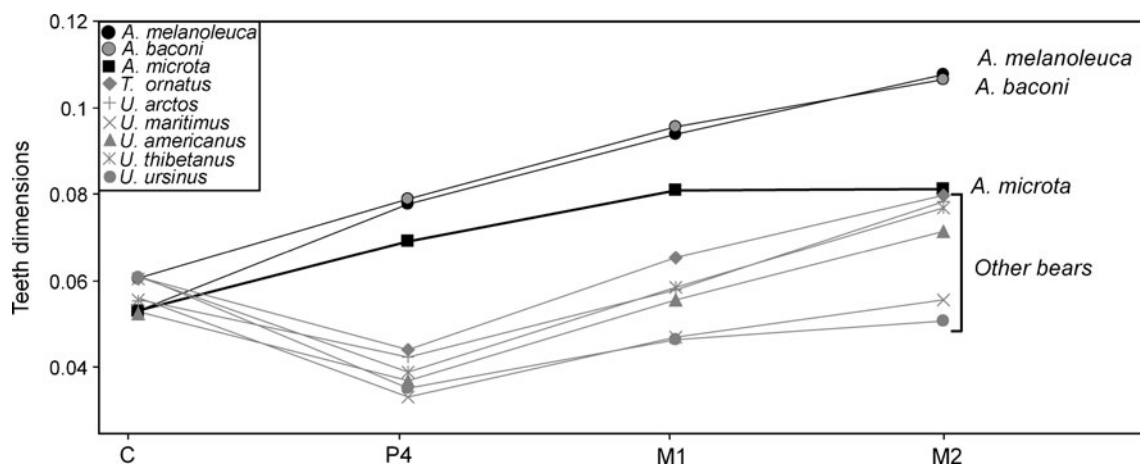


Fig. 5 Relative dimensions of upper teeth in extant bears and extinct ailuropodines, estimated averaging the maximal anteroposterior and lateromedial diameters of all specimens per species. Points represent the square root of the anteroposterior diameter multiplied by the

lateromedial one of each tooth, divided by skull length. C canine, P4 fourth premolar, M1 first molar (carnassial), M2 second molar. Note that *U. malayanus* was not included here for clarity, given its highly developed canines

(e.g., bamboo plants) in bears (Figueirido et al. 2009, 2010; Figueirido and Soiblezon 2010). However, it is worth noting that although the adaptations for durophagy are also evidenced in carnivores by well-distinctive mandible shapes (Werdelin 1989; Meloro et al. 2008), the absence of fossil jaws of *A. microta* precluded us from analyzing the tempo and mode in which these adaptations were achieved in ailuropodines.

Therefore, our results suggest that the specialized diet of *A. melanoleuca* was already present in *A. microta* during late Pliocene times. However, the cranium is broader over the postorbital process and the zygomatic arches in the pygmy panda than in both the living and Pleistocene giant pandas. This implies that the area in the temporal fossa of the cranium of *A. microta* for insertion of the temporalis muscle was comparatively smaller than in other ailuropodines. As a result, a gradual development of this muscle from *A. microta* through *A. baconi* to *A. melanoleuca* was achieved. Given that the temporalis is one of the main muscles involved in mastication (Ewer 1973), *A. microta* most probably had a lesser bite force than *A. melanoleuca*. However, it is possible that the increase in size of the temporalis muscle resulted from allometric effects because the pygmy panda was considerably smaller than the living *A. melanoleuca* (Jin et al. 2007). However, the fact that the late Pleistocene *A. baconi* was larger than the living giant panda and had a narrower braincase over the postorbital process suggests that the gradual development of the temporalis muscle through the evolution of the *Ailuropoda* lineage was not merely an artifact resulting from scaling effects. In addition, the more posteriorly flexed occipital region of *A. microta* compared to *A. melanoleuca* indicates that the living panda experienced a verticalization of the temporalis muscle fibers. It is worth noting that a similar pattern was also achieved, although to a more extreme degree, in a very different evolutionary context by the highly specialized hypercarnivorous saber-toothed cats. Given the extreme elongation of their upper canine teeth, these predators had the need of maximizing the opening of the mouth. This was achieved by the verticalization of the temporalis muscle, which diminished fiber stretch with retention of a powerful bite force at the carnassial (Emerson and Radinsky 1980). For this reason, the verticalized occiput of the giant panda probably represents an adaptation for delivering strong bite forces when thick bamboo stems are placed at the posterior molars. The less verticalized occiput of *A. microta* might indicate that, despite a tough fibrous diet in the pygmy panda, it did not utilize bamboo stems as the giant panda does. In addition, the pygmy giant panda has a second upper molar less developed than in the giant panda, which probably indicates a reduced ability for processing tough foods. This is also in agreement with the smaller bite force of the

Pliocene species and could be tentatively interpreted as evidencing that *A. microta* consumed a greater fraction of the less fibrous parts of bamboo plants (e.g., leaves, shoots, and fruits), as the red panda (*Ailurus fulgens*) does today (Chorn and Hoffmann 1978).

Our results show that cranial shape was modified in the giant panda lineage from the most plesiomorphic state of the ancestral Miocene *Ursavus*, probably by selective forces favoring the consumption of tough foods like bamboo (Jin et al. 2007). However, the fact that only two extinct species could be included in this morphometric study precludes us from drawing strong inferences on the pace of morphological change in *Ailuropoda* (e.g., the evolutionary rate of each skull trait and the role of allometric scaling). Only future findings in the fossil record could provide crucial insights into the timing of skull transformation in the panda's lineage.

Acknowledgements We thank Eileen Westwig (AMNH, New York), Roberto Portela, Louise Tomsett, and Paula Jenkins (NHM, London) for kindly providing access to the collections under their care. This work has been supported by the research projects of the Ministry of Science and Innovation to P.P. and J.A.P.C. (CGL2006-13808-C02-02 and CGL2008-04896) by a research project of the Chinese National Natural Science Foundation (No. 40772014) to W. D. and a F.P.U. Ph.D. research grant to B. F.

References

- Bininda-Emonds ORP (2004) Phylogenetic position of the giant panda: historical consensus through supertree analysis. In: Lindburg D, Baragona K (eds) Giant pandas, biology and conservation. University of California Press, California, pp 11–35
- Bininda-Emonds ORP, Gittleman JL, Purvis A (1999) Building large trees by combining phylogenetic information: a complete phylogeny of extant Carnivora (Mammalia). *Biol Rev* 74:143–175
- Chorn J, Hoffmann RS (1978) *Ailuropoda melanoleuca*. *Mamm Species* 110:1–6
- Christiansen P (2007) Evolutionary implications of bite mechanics and feeding ecology in bears. *J Zool Lond* 272:423–443
- Dong W (2008) Virtual cranial endocast of the oldest giant panda (*Ailuropoda microta*) reveals great similarity to that of its extant relative. *Naturwissenschaften* 95:1079–1083
- Drake AG, Klingenberg CP (2008) The pace of morphological change: historical transformation of skull shape in St Bernard dogs. *Proc R Soc B* 275:71–76
- Dryden IL, Mardia K (1998) *Statistical shape analysis*. Wiley, Chichester
- Emerson SB, Radinsky L (1980) Functional analysis of sabertooth cranial morphology. *Paleobiology* 6:295–312
- Ewer RF (1973) *The carnivores*. Cornell University Press, New York
- Figueirido B, Soiblezon LH (2010) Inferring palaeoecology in extinct tremarctine bears (Carnivora, Ursidae) using geometric morphometrics. *Lethaia* 43:209–222
- Figueirido B, Palmqvist P, Pérez-Claros JA (2009) Ecomorphological correlates of craniodental variation in bears and palaeobiological

- implications for extinct taxa: an approach based on geometric morphometrics. *J Zool Lond* 277:70–80
- Figueirido B, Pérez-Claros JA, Torregrosa V, Martín-Serra A, Palmqvist P (2010) Demythologizing *Arctodus simus*, the ‘short-faced’ long-legged, and predaceous bear that never was. *J Vertebr Paleontol* 30:262–275
- Flynn JJ, Nedbal M (1998) Phylogeny of the Carnivora (Mammalia): congruence vs incompatibility among multiple data sets. *Mol Phylogenet Evol* 9:414–426
- Gittleman JL (1994) Are the pandas successful specialists or evolutionary failures? *Bioscience* 44:456–464
- Gower JC (1975) Generalized procrustes analysis. *Psychometrika* 40:33–51
- Hunt RM Jr (2004) A paleontologist's perspective on the origin and relationships of the giant panda. In: Lindburg D, Baragona K (eds) *Giant pandas, biology and conservation*. University of California Press, California, pp 45–52
- Jin C, Ciochon RL, Dong W, Hunt RM, Jr LJ, Jaeger M, Zhu Q (2007) The first skull of the earliest giant panda. *Proc Natl Acad Sci USA* 104:10932–10937
- Klingenberg CP (2011) MorphoJ: an integrated software package for geometric morphometrics. *Mol Ecol Resour*. doi:10.1111/j.1755-998.2010.02924.x
- Klingenberg CP, Barluenga M, Meyer A (2002) Shape analysis of symmetric structures: quantifying variation among individuals and asymmetry. *Evolution* 56:1909–1920
- Krause J, Unger T, Noçon A et al (2008) Mitochondrial genomes reveal an explosive radiation of extinct and extant bears near the Miocene-Pliocene boundary. *BMC Evol Biol* 8:220
- Meloro C, Raia P, Piras P et al (2008) The shape of the mandibular corpus in large fissiped carnivores: allometry, function and phylogeny. *Zool J Linn Soc* 154:832–845
- Monteiro LR (1999) Multivariate regression models and geometric morphometrics: the search for causal factors in the analysis of shape. *Syst Biol* 48:192–199
- Qi G, Dong W, Zheng L, Zhao L, Gao F, Yue L, Zhang Y (2006) Taxonomy, age and environment status of the Yuanmou hominoids. *Chinese Sci Bull* 51:704–712
- Qiu ZX, Qi G (1989) Ailuropod found from the late Miocene deposits in Lufeng, Yunnan. *Vertebrata Palasiatica* 27:153–169
- Rohlf FJ (2006) TpsDig, ver. 2.05. Department of Ecology and Evolution, State University of New York at Stony Brook, Stony Brook
- Sacco T, Van Valkenburgh B (2004) Ecomorphological indicators of feeding behaviour in the bears (Carnivora: Ursidae). *J Zool Lond* 263:41–54
- Slater GJ, Van Valkenburgh B (2008) Long in the tooth: evolution of sabertooth cat cranial shape. *Paleobiology* 34:403–419
- Werdelin L (1989) Constraint and adaptation in the bone-cracking canid *Osteoborus* (Mammalia: Canidae). *Paleobiology* 15:387–401
- Wyss AR, Flynn JJ (1993) A phylogenetic analysis and definition of the Carnivora. In: Szalay FS, Novacek MJ, Mckenna MC (eds) *Mammal phylogeny: placentals*. Springer, New York, pp 32–52
- Zhang S, Pan R, Li M, Oxnard C, Wei F (2007) Mandible of the giant panda (*Ailuropoda melanoleuca*) compared with other Chinese carnivores: functional adaptation. *Biol J Linn Soc* 92:449–456